RAPID COMMUNICATION

Nonreciprocal negative refraction in a dense hot atomic medium

Hai Yi(易海)[1,2], Hongjun Zhang(张红军)[1,2,†], and Hui Sun(孙辉)[1,2]

[1] *School of Physics and Information Technology, Shaanxi Normal University, Xi'an* 710119, *China*
[2] *Xi'an Key Laboratory of Optical Information Manipulation and Augmentation, Xi'an* 710119, *China*

(Received 1 November 2022; revised manuscript received 18 December 2022; accepted manuscript online 27 December 2022)

We investigate the electromagnetic properties of a four-level dense atomic gas medium with Doppler effect. It is shown that the relative permittivity and relative permeability of the medium can be negative simultaneously with low absorption in the same detuning interval on account of electromagnetically induced transparency. Furthermore, with the suitable parameters, the nonreciprocal negative refraction can be obtained due to the Doppler effect, and the nonreciprocity frequency band can be regulated by adjusting the temperature, the intensity of the control field and the atomic density in this hot atomic medium.

Keywords: negative refraction, nonreciprocity, Doppler effect, atomic system

PACS: 42.25.Bs, 43.28.Py, 51.70.+f, 78.20.Ci **DOI:** 10.1088/1674-1056/acae7a

1. Introduction

Nonreciprocal devices are essential components in quantum information processing such as optical isolators[1–4] and optical circulators.[5–8] Their basic principle is optical nonreciprocity which means that the light field has different transmission characteristics in two opposite propagation directions. The realization of nonreciprocity lies in breaking the Lorentz reciprocity. Generally, the traditional route to break the Lorentz reciprocity is employing the magneto-optical Faraday effect.[9,10] It needs bulky magnets to generate strong magnetic field, which brings difficulty to devices miniaturization. Compared with the traditional route, magnetic-free optical nonreciprocity has more advantages in miniaturization. In recent years, many theoretical schemes have been suggested to obtain non-magnetic nonreciprocity, such as nonlinear effects,[11–14] time-space regulation of dielectric constant,[15–18] optomechanical systems,[19–22] moving atomic lattices,[23–26] chiral quantum systems,[27–30] and hot atoms systems.[31–34] It has also been realized in experiments with remarkable results.[35–38]

Moreover, in recent decades, negative refraction materials (NIMs) have also attracted extensive attention of the researchers because of their surprising and counter-intuitive properties including the reversal Doppler shift, reversal Cherenkov effect,[39] negative Goos–Hänchen shift,[40] evanescent wave amplification,[41] and subwavelength focusing.[41–43] In these materials, the relative permittivity and permeability are negative simultaneously,[39] so that the electric field strength E'', the magnetic induction strength B'' and the propagation vector k'' follow the left-hand rule, so they are also called left-handed materials (LHMs). A well-known potential application of NIMs is "perfect lens", which can break through the diffraction limit in imaging resolution.[44] Meanwhile, negative refraction materials can also be used to make "invisibility cloak" which can make objects completely invisible.[45] However, NIMs do not exist in nature. Up to now, there are several approaches to obtain NIMs, including composite metamaterials,[46–50] photonic crystal structures,[51–55] chiral material[56–58] and coherent atomic vapor.[59–63] The former three methods belong to adjustment and control of structure, which need complex structure manufacturing technique. While the latter mechanism is external field manipulation and quantum coherence, it does not need a complex structure and the material is isotropic and homogeneous, so it has some advantages in the realization of NIMs.[60]

Quantum coherence approach to obtain negative refractive index was first proposed by Oktel *et al*. and Shen *et al*. in 2004.[59,60] They found that it was possible to achieve negative refractive index due to quantum coherence in dense Lambda-type atomic gases. However, it requires rigorous atomic level condition. Generally speaking, the strength of magnetic dipole moment is usually α^2 weaker than the strength electric dipole moment so that it is very difficult to change the magnetic permeability in common atomic system. In order to get large electric and magnetic responses simultaneously, the electric-dipole transition and the magnetic-dipole transition need to occur at the same time.[59] In other words, the level energy difference corresponding to the electric-dipole transition should be approximately equal to that of magnetic-dipole transition. In order to overcome this limit, Thommen and his colleague put forward a four-level atomic scheme based on electromagnetic induction transparency (EIT) to realize negative refraction in

[†]Corresponding author. E-mail: zhhjun@snnu.edu.cn

© 2023 Chinese Physical Society and IOP Publishing Ltd

2006.[63] Subsequently, Fleischhauer *et al.* used electromagnetic induced chirality to realize negative refraction in a five-level atomic system.[64] Later, more schemes to realize negative refraction with low absorption were proposed based on EIT.[65–68]

Motivated by the idea of the nonreciprocity induced by Doppler effect and negative refraction based on quantum coherence, we propose a nonreciprocal negative refraction scheme in hot atomic gas medium. Nonreciprocal negative refraction refers to that light behaves negative refraction when it incidences in one direction while behaves normal refraction property in the opposite direction. It is well known that negative refraction will lead to light completely bypassing obstacles in one direction,[45] which can make the object invisible, on the other hand, light will be completely blocked in the opposite direction so that the object can be seen if nonreciprocal negative refraction occurs. Our aim is to extend nonreciprocal devices to the negative refraction materials and to realize invisible effect in single direction by nonreciprocal negative refraction.

In our paper, we present a hot four-level atomic system and use the electric and magnetic components of the probe field to couple electric dipole transition and magnetic dipole transition simultaneously.[59,63] We find that the relative permittivity and relative permeability of the medium can be negative at the same time in some frequency band based on EIT. In our scheme, the physical mechanism leading to the nonreciprocal negative refraction is the difference of the Doppler shifts in forward and backward probe propagation directions. Due to the difference of the Doppler shifts, the forward and the backward propagations of the probe field have different refraction properties. Under appropriate condition, the negative refraction can be obtained in one direction but normal refraction occurs in the opposite direction. Therefore, we can realize the nonreciprocal negative refraction and the nonreciprocal negative refraction frequency band can be controlled by the temperature, the intensity of the control field and atomic density in this hot atomic gaseous medium.

2. Theoretical model

We consider a four-level system interacting with three coherent optical fields as shown in Fig. 1. The two lower energy levels $|2\rangle$ and $|1\rangle$ have the same parity, then the transition from $|2\rangle$ to $|1\rangle$ is electric-dipole forbidden, but magnetic dipole transition (with magnetic dipole moment $\boldsymbol{\mu}_{12} = \langle 1|\boldsymbol{\mu}|2\rangle \neq 0$) is allowed. The energy levels $|3\rangle$ and $|4\rangle$ have opposite parity, then electric dipole transition $|3\rangle \leftrightarrow |4\rangle$ (with electric dipole moment $\boldsymbol{d}_{34} = \langle 3|\boldsymbol{d}|4\rangle \neq 0$) is allowed. In our scheme, the transitions $|3\rangle \leftrightarrow |4\rangle$ and $|1\rangle \leftrightarrow |2\rangle$ are nearly degenerate, then we introduce a probe field with frequency $\omega_{\rm p}$ to couple the two transitions at the same time and the corresponding Rabi frequencies are $\Omega_{\rm p}^{E} = \boldsymbol{d}_{34}\cdot\boldsymbol{E}/\hbar$ and $\Omega_{\rm p}^{B} = \boldsymbol{\mu}_{12}\cdot\boldsymbol{B}/\hbar$, where $\boldsymbol{E}$ and $\boldsymbol{B}$ are the electric field and magnetic field components of the probe field. Two control fields with frequencies ω_{13} (Rabi frequency Ω_{13}) and ω_{24} (Rabi frequency Ω_{24}) couple the transitions $|1\rangle \leftrightarrow |3\rangle$ and $|2\rangle \leftrightarrow |4\rangle$, and the transition $|1\rangle \leftrightarrow |3\rangle$ is a two-photon process.

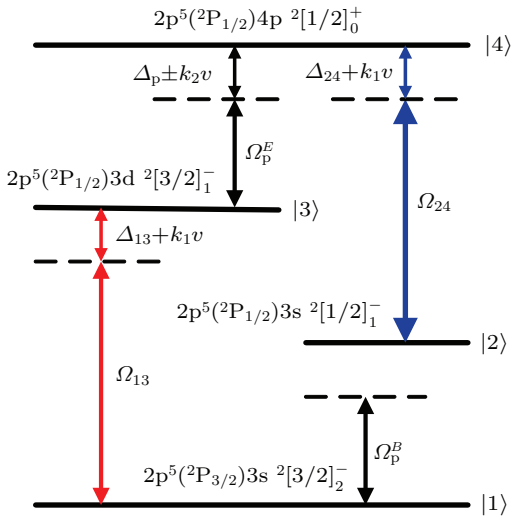


Fig. 1. Scheme diagram of four-level atomic medium interacting with control fields Ω_{24}, Ω_{13} and probe field $\Omega_{\rm p}$ (Ω_i stands for the Rabi frequency of electric and magnetic dipole transitions by probe field).

In interaction picture, with the dipole approximation and rotating-wave approximation, the interaction Hamiltonian is given as

$$\begin{aligned} H \;=\; & \hbar[(\Delta_{13}+\Delta_{\rm p}-\Delta_{24})\,|2\rangle\langle 2| \\ & +\Delta_{13}\,|3\rangle\langle 3| + (\Delta_{13}+\Delta_{\rm p})\,|4\rangle\langle 4|] \\ & -\hbar(\Omega_{13}\,|1\rangle\langle 3| + \Omega_{24}\,|2\rangle\langle 4| \\ & +\Omega_{\rm p}^{E}\,|3\rangle\langle 4| + \Omega_{\rm p}^{B}\,|1\rangle\langle 2| + {\rm h.c.}). \end{aligned} \tag{1}$$

Using the density matrix approach, the time-evolution of the system is written as

$$\frac{{\rm d}\rho}{{\rm d}t} = -\frac{\rm i}{\hbar}[H,\rho] + \Lambda\rho, \tag{2}$$

where $\Lambda\rho$ is the damping term of the coherence, and the equations of density matrix elements are

$$\begin{aligned} \dot{\rho}_{11} \;=\; & {\rm i}\Omega_{12}(\rho_{21}-\rho_{12}) + {\rm i}\Omega_{13}(\rho_{31}-\rho_{13}) \\ & +\gamma_{21}\rho_{22}+\gamma_{31}\rho_{33}, \end{aligned} \tag{3a}$$

$$\begin{aligned} \dot{\rho}_{22} \;=\; & {\rm i}\Omega_{12}(\rho_{12}-\rho_{21}) + {\rm i}\Omega_{24}(\rho_{42}-\rho_{24}) \\ & -\gamma_{21}\rho_{22}+\gamma_{42}\rho_{44}, \end{aligned} \tag{3b}$$

$$\begin{aligned} \dot{\rho}_{33} \;=\; & {\rm i}\Omega_{13}(\rho_{13}-\rho_{31}) + {\rm i}\Omega_{34}(\rho_{43}-\rho_{34}) \\ & -\gamma_{31}\rho_{33}+\gamma_{43}\rho_{44}, \end{aligned} \tag{3c}$$

$$\begin{aligned} \dot{\rho}_{44} \;=\; & {\rm i}\Omega_{24}(\rho_{24}-\rho_{42}) + {\rm i}\Omega_{34}(\rho_{34}-\rho_{43}) \\ & -\gamma_{42}\rho_{44}-\gamma_{43}\rho_{44}, \end{aligned} \tag{3d}$$

$$\begin{aligned} \dot{\rho}_{21} \;=\; & {\rm i}\delta_{21}\rho_{21} + {\rm i}\Omega_{12}\rho_{11} - {\rm i}\Omega_{12}\rho_{22} \\ & -{\rm i}\Omega_{13}\rho_{23} + {\rm i}\Omega_{24}\rho_{41}, \end{aligned} \tag{3e}$$

$$\dot{\rho}_{31} = \mathrm{i}\delta_{31}\rho_{31} + \mathrm{i}\Omega_{13}\rho_{11} - \mathrm{i}\Omega_{13}\rho_{33} - \mathrm{i}\Omega_{12}\rho_{32} + \mathrm{i}\Omega_{34}\rho_{41}, \tag{3f}$$

$$\dot{\rho}_{41} = \mathrm{i}\delta_{41}\rho_{41} - \mathrm{i}\Omega_{12}\rho_{42} - \mathrm{i}\Omega_{13}\rho_{43} + \mathrm{i}\Omega_{24}\rho_{21} + \mathrm{i}\Omega_{34}\rho_{31}, \tag{3g}$$

$$\dot{\rho}_{32} = \mathrm{i}\delta_{32}\rho_{32} - \mathrm{i}\Omega_{12}\rho_{31} + \mathrm{i}\Omega_{13}\rho_{12} - \mathrm{i}\Omega_{24}\rho_{34} + \mathrm{i}\Omega_{34}\rho_{42}, \tag{3h}$$

$$\dot{\rho}_{42} = \mathrm{i}\delta_{42}\rho_{42} - \mathrm{i}\Omega_{12}\rho_{41} + \mathrm{i}\Omega_{24}\rho_{22} - \mathrm{i}\Omega_{24}\rho_{44} + \mathrm{i}\Omega_{34}\rho_{32}, \tag{3i}$$

$$\dot{\rho}_{43} = \mathrm{i}\delta_{43}\rho_{43} - \mathrm{i}\Omega_{13}\rho_{41} + \mathrm{i}\Omega_{24}\rho_{23} - \mathrm{i}\Omega_{34}\rho_{44} + \mathrm{i}\Omega_{34}\rho_{33}, \tag{3j}$$

where γ_{ij} is the spontaneous emission decay rate from level $|i\rangle$ to level $|j\rangle$, $\delta_{21} = \Delta_{24} - \Delta_\mathrm{p} - \Delta_{13} + \mathrm{i}\Gamma_{21}$, $\delta_{31} = -\Delta_{13} + \mathrm{i}\Gamma_{31}$, $\delta_{32} = \Delta_\mathrm{p} - \Delta_{24} + \mathrm{i}\Gamma_{32}$, $\delta_{43} = -\Delta_\mathrm{p} + \mathrm{i}\Gamma_{43}$, $\delta_{42} = -\Delta_{24} + \mathrm{i}\Gamma_{42}$, and $\delta_{41} = -\Delta_{13} - \Delta_\mathrm{p} + \mathrm{i}\Gamma_{41}$. Here, the detunings of the applied fields are defined as $\Delta_{13} = \omega_{13} - (\varepsilon_3 - \varepsilon_1)/\hbar$, $\Delta_{24} = \omega_{24} - (\varepsilon_4 - \varepsilon_2)/\hbar$, $\Delta_\mathrm{p} = \omega_\mathrm{p} - (\varepsilon_4 - \varepsilon_3)/\hbar$. Γ_{ij} is the damping rate of the coherence, $\Gamma_{21} = \gamma_{21}/2$, $\Gamma_{31} = \gamma_{31}/2$, $\Gamma_{32} = (\gamma_{31} + \gamma_{21})/2$, $\Gamma_{41} = (\gamma_{43} + \gamma_{42})/2$, $\Gamma_{43} = (\gamma_{43} + \gamma_{42} + \gamma_{31})/2$, and $\Gamma_{42} = (\gamma_{43} + \gamma_{42} + \gamma_{21})/2$. For simplification and without loss of generality, we set the Rabi frequency Ω_{ij} to be real and the density matrix elements satisfy the closed conditions $\rho_{11} + \rho_{22} + \rho_{33} + \rho_{44} = 1$ and $\rho_{ij}^* = \rho_{ji}$.

We assume that the atoms are all populated at the level $|1\rangle$ initially, the probe field Ω_p^E and the control field Ω_{13} are weak coherence fields, while the control field Ω_{24} is strong coherence field, and the relationship between them is $\Omega_\mathrm{p}^E \ll \Omega_{13} < \Omega_{24}$. In this way, the Liouville equation can be solved in the steady state, and the expressions of the density matrix elements are obtained as

$$\rho_{21} = -\frac{\delta_{41}\rho_{11}^{(0)}\Omega_{12} - \rho_{31}^{(0)}\Omega_{24}\Omega_{34}}{\delta_{21}\delta_{41} - \Omega_{24}^2}, \tag{4}$$

$$\rho_{43} = -\frac{\left(\delta_{21}\delta_{23}\left(\delta_{41}\rho_{33}^{(0)} + \rho_{31}^{(0)}\Omega_{13}\right) + \left(-\delta_{23}\rho_{33}^{(0)} + \rho_{31}^{(0)}\Omega_{13}\right)\Omega_{24}^2\right)\Omega_{34}}{\left(\delta_{21}\delta_{41} - \Omega_{24}^2\right)\left(\delta_{23}\delta_{43} - \Omega_{24}^2\right)} + \frac{\Omega_{12}\Omega_{24}\left(\delta_{21}\delta_{41}\rho_{13}^{(0)} + (\delta_{23} + \delta_{41})\rho_{11}^{(0)}\Omega_{13} - \rho_{13}^{(0)}\Omega_{24}^2\right)}{\left(\delta_{21}\delta_{41} - \Omega_{24}^2\right)\left(\delta_{23}\delta_{43} - \Omega_{24}^2\right)}, \tag{5}$$

where

$$\rho_{11}^{(0)} = \frac{\gamma_{31}\delta_{13}\delta_{31} + \mathrm{i}(\delta_{31} + \delta_{13})\Omega_{13}^2}{\gamma_{31}\delta_{13}\delta_{31} + 2\mathrm{i}(\delta_{13} + \delta_{31})\Omega_{13}^2}, \tag{6a}$$

$$\rho_{33}^{(0)} = \frac{\mathrm{i}(\delta_{13} + \delta_{31})\Omega_{13}^2}{\gamma_{31}\delta_{13}\delta_{31} + 2\mathrm{i}(\delta_{13} + \delta_{31})\Omega_{13}^2}, \tag{6b}$$

$$\rho_{13}^{(0)} = \frac{\gamma_{31}\delta_{31}\Omega_{13}}{\gamma_{31}\delta_{13}\delta_{31} + 2\mathrm{i}(\delta_{13} + \delta_{31})\Omega_{13}^2}, \tag{6c}$$

$$\rho_{31}^{(0)} = -\frac{\gamma_{31}\delta_{13}\Omega_{13}}{\gamma_{31}\delta_{13}\delta_{31} + 2\mathrm{i}(\delta_{13} + \delta_{31})\Omega_{13}^2}, \tag{6d}$$

in which $\delta_{13} = \Delta_{13} + \mathrm{i}\Gamma_{31}$.

As the Doppler effect is considered, the detunings of the applied fields in the above equations should be changed. In our scheme, the two control fields always propagate forward, the detunings are replaced by $\Delta_{13}^* = \Delta_{13} + k_1\upsilon$, $\Delta_{24}^* = \Delta_{24} + k_1\upsilon$. For the probe field, when it propagates forward, the detuning is replaced by $\Delta_\mathrm{p}^\mathrm{F} = \Delta_\mathrm{p} + k_2\upsilon$, while it propagates backward, the detuning is replaced by $\Delta_\mathrm{p}^\mathrm{B} = \Delta_\mathrm{p} - k_2\upsilon$, where $k_1 = 2\pi/\lambda_1$, $k_2 = 2\pi/\lambda_2$, and λ_i stands for the wavelength of the applied fields.

It is well known that the electric response of the atomic medium to the probe field depends on the coherence term ρ_{43}, and the atomic electric dipole moment can be given by $\boldsymbol{P}(\omega_\mathrm{p}) = \mathrm{Tr}\{\hat{\rho}\hat{\boldsymbol{d}}\} = \rho_{43}\boldsymbol{d}_{34}$. Besides, according to the classic theory, the atomic polarizability is obtained by $\boldsymbol{P}(\omega_\mathrm{p}) = \varepsilon_0\alpha_\mathrm{e}(\omega_\mathrm{p})\boldsymbol{E}(\omega_\mathrm{p})$. For simple calculation, we make the electric field $\boldsymbol{E}(\omega_\mathrm{p})$ parallel to the atomic electric dipole moment $\boldsymbol{d}_{34}$, so α_e is a scalar, and the electric polarizability can be expressed as

$$\alpha_\mathrm{e} = \frac{\rho_{43}d_{34}}{\varepsilon_0 E}. \tag{7}$$

Similarly, the magnetic response of the atomic medium to the probe field depends on the coherence term ρ_{21}, and the magnetization is given by $\boldsymbol{M}(\omega_\mathrm{p}) = \mathrm{Tr}\{\hat{\rho}\hat{\boldsymbol{\mu}}\} = \rho_{21}\boldsymbol{\mu}_{12}$. In addition, according to the classic theory, the atomic magnetizability is obtained by $\mu_0\boldsymbol{M}(\omega_\mathrm{p}) = \alpha_\mathrm{m}(\omega_\mathrm{p})\boldsymbol{B}(\omega_\mathrm{p})$. In the case that the atomic magnetic dipole moment $\boldsymbol{\mu}_{12}$ and the magnetic field $\boldsymbol{B}(\omega_\mathrm{p})$ are parallel, the atomic magnetic susceptibility α_m is also a scalar and can be expressed as

$$\alpha_\mathrm{m} = \frac{\mu_0\rho_{21}\mu_{12}}{B}. \tag{8}$$

In a hot atomic medium, the thermal motion of the atoms cannot be ignored. In the case of considering the thermal motion of the atoms and the input of a strong control field, the magnetic susceptibility of the atoms is chiral and it will generate different Doppler frequency shifts to the probe field to realize optical nonreciprocity.[34]

The atomic polarizability and magnetic susceptibility with the Doppler effect can be obtained by[37]

$$\chi = \int_{-\infty}^{+\infty} N(\upsilon)\,\alpha(\upsilon)\,\mathrm{d}\upsilon, \tag{9}$$

where $N(\upsilon) = N\mathrm{e}^{-\upsilon^2/\upsilon_\mathrm{p}^2}/(\upsilon_\mathrm{p}\sqrt{\pi})$ with υ_p the most probable speed of the atoms and atomic density N, and $\alpha(\upsilon)$ is the atomic polarizability or atomic magnetic susceptibility.

Generally, people focus on the macroscopic physical quantities of the medium. In a dense gas medium, the local field effect should be considered. According to the Clausius–Mossotti relationship,[69] the relative permittivity and the relative permeability of the medium are expressed as

$$\varepsilon_\mathrm{r} = \frac{1+\frac{2}{3}\chi_\mathrm{e}}{1-\frac{1}{3}\chi_\mathrm{e}}, \tag{10a}$$

$$\mu_\mathrm{r} = \frac{1+\frac{2}{3}\chi_\mathrm{m}}{1-\frac{1}{3}\chi_\mathrm{m}}. \tag{10b}$$

3. Results and discussion

In this section, we will investigate the negative refraction property of this hot atomic medium to the probe field in forward and backward direction based on the above analytical solution. We choose neon atoms to verify our scheme, and the atomic parameters are selected as follow: the electric dipole moment is $|\boldsymbol{d}_{34}| = 10^{-29}$ C, the magnetic dipole moment is $|\boldsymbol{\mu}_{12}| = 9.274\times10^{-24}$ C$\cdot$m$^2\cdot$s^{-1},[63] the wavelengths of the control field and probe field are $\lambda_1 = 352$ nm and $\lambda_2 = 5.4$ μm. We set the spontaneous radiation decay rate from excited state $|3\rangle$ to the ground state $|1\rangle$ to the unit reference $\gamma_{31} = \gamma = 10^8$ s^{-1}, and the parameters are scaled by γ. The other decay rates are chosen as $\gamma_{42} = \gamma_{43} = \gamma$, $\gamma_{21} = \gamma\cdot\alpha^2$, where $\alpha = 1/137$ is the fine structure constant.

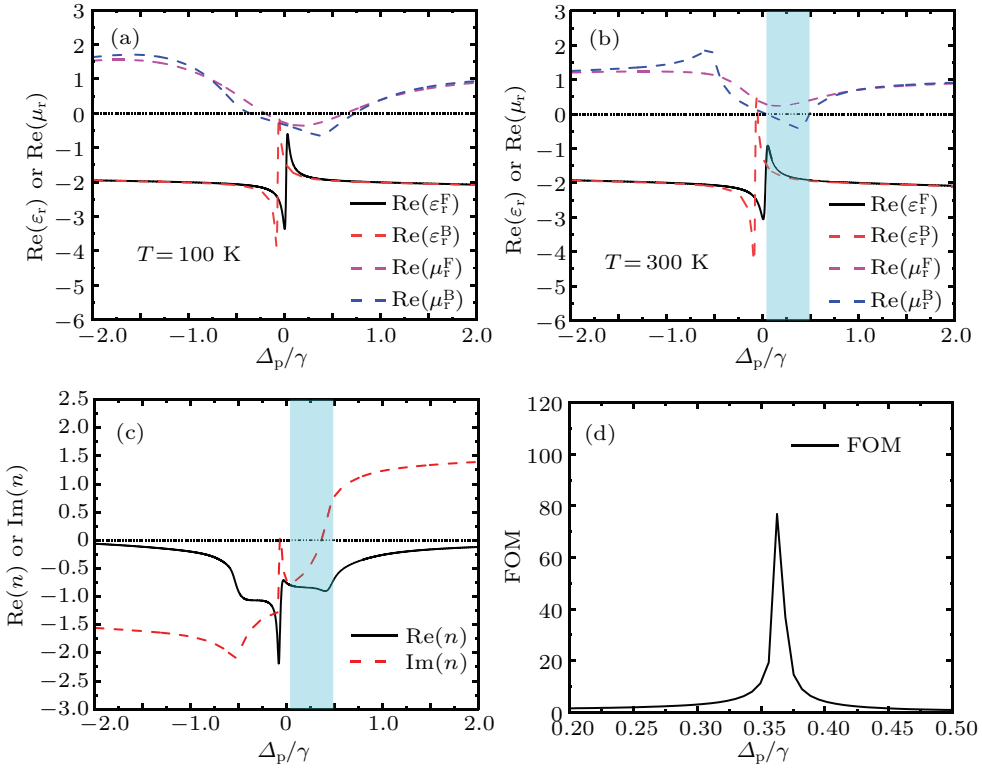


Fig. 2. The real part of the forward relative permittivity (black solid line) and permeability (magenta dotted line), the real part of the backward relative permittivity (red dashed line) and permeability (blue dash dot line) as a function of probe field detuning at different temperatures: (a) $T = 100$ K, (b) $T = 300$ K. (c) The real part (black solid line) and the imaginary part (red dashed line) of the refractive index, and (d) the FOM as a function of probe field detuning in backward direction when the temperature $T = 300$ K. The shaded area represents the nonreciprocal negative refraction interval. The other parameters are selected as $\gamma_{31} = \gamma_{42} = \gamma_{43} = \gamma = 10^8$ s^{-1}, $\gamma_{21} = \gamma\cdot\alpha^2$, $\alpha = 1/137$, $\Omega_{24} = 1.0\gamma$, $\Omega_{13} = 0.15\gamma$, $N = 1.5\times10^{25}$ at/m^3, $\Delta_{13} = \Delta_{24} = 1.0\gamma$.

First, we analyze the negative refraction property of the medium to the probe field at different temperatures. In order to get the maximum electric and magnetic responses, we set $\Delta_{13} = \Delta_{24} = 1.0\gamma$ to satisfy he EIT condition. The parameters are selected as $\Omega_{24} = 1.0\gamma$, $\Omega_{13} = 0.15\gamma$, $N = 1.5\times10^{25}$ at/m^3, and other parameters as shown above. Figure 2 plots the temperature dependence of the electromagnetic properties of the medium on different probe field detunings for the forward and backward propagation cases. As shown in Fig. 2(a), when the temperature is low, both of the relative permeability and relative permittivity of the forward and backward directions are negative in an extent frequency band. It is to say that negative refraction exists in both propagation directions. It is easy to understand with the negative refraction induced by EIT.[63] As we know, the Doppler shift is very small at low temperature and the EIT conditions still satisfy in both directions. The electric and magnetic components of the probe field are simultaneously applied to the transitions $|3\rangle \leftrightarrow |4\rangle$ and $|1\rangle \leftrightarrow |2\rangle$ respectively, then the absorption is strongly suppressed by EIT, and the medium stores a large

amount of energy in the process of interaction, resulting in a strong response of the material.[59] So the relative permeability and relative permittivity can be changed to be negative at the same time in both propagation directions. Then the negative refraction occurs due to EIT at low temperature in both directions. Meanwhile, when the temperature becomes high, we find that the medium exhibits different electromagnetic properties in the forward and backward cases as shown in Fig. 2(b). It is shown that the relative permeability of the forward case is positive while both of the relative permeability and permittivity are still negative in the backward case. Hence, the negative refraction exists only in the backward case. It means that the nonreciprocal negative refraction is realized when the temperature is high enough. It is because the Doppler shift becomes large with the increasing temperature, and the Doppler shifts of the probe field are opposite to the cases of the forward and backward propagation directions. As for the forward case, the Doppler effect simultaneously enhances the detunings of all the fields. However, in the backward probe field propagation case, the Doppler effect enhances the detunings of the control fields but weakens the detuning of the probe field. Hence, in the forward case, the EIT condition is broken, then the electromagnetic response of the medium gets weak and it is difficult to realize negative refraction. Compared with the forward propagation, the atomic system is close to the EIT state in the backward case and the medium still exhibits strong macroscopic polarization and magnetization. Therefore, the medium has different negative refraction properties in forward and backward directions.

In order to ensure that the negative refraction really exists, the absorption of the medium must be small in the refraction band. Generally, researchers use the figure of merit (FOM) to measure the quality of the negative refraction. The FOM is defined as $\mathrm{Re}[n]/\mathrm{Im}[n]$.[67] Then we study the negative refraction with FOM corresponding to the case of Fig. 2(b) in the backward case. As shown in Fig. 2(c), we find that the refractive index is negative and the absorption is very small. From Fig. 2(d), it is shown that the FOM is much larger than 1 in the nonreciprocal negative refraction range. In other words, the negative refraction with less absorption is realized in backward propagation. It may guarantee that the nonreciprocal negative refraction is really obtained in our scheme.

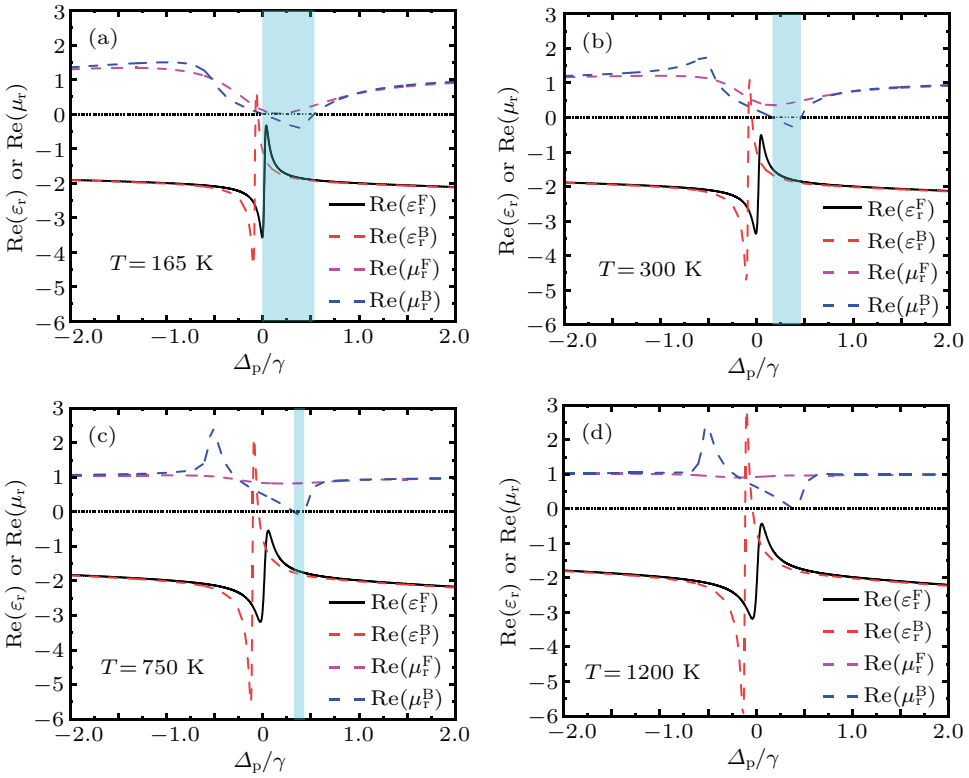


Fig. 3. The real part of the forward relative permittivity (black solid line) and permeability (magenta dotted line), the real part of the backward relative permittivity (red dashed line) and permeability (blue dash dot line) as a function of probe field detuning at different temperatures: (a) $T = 165$ K, (b) $T = 300$ K, (c) $T = 750$ K, (d) $T = 1200$ K. The shaded area represents the nonreciprocal negative refraction interval. The parameters are selected as $\Omega_{13} = 0.12\gamma$, and the other parameters are the same as those in Fig. 2.

Next, we discuss the temperature effect on the nonreciprocal negative refraction properties of the medium. The temperature range is given from 165 K to 1200 K. Figure 3 shows the dependence of the real parts of the relative permittivity and permeability of the medium for the forward and backward probe field propagation with different temperatures. The parameters are selected as $\Omega_{13} = 0.12\gamma$ and the other parameters are the same as those in Fig. 2. We find that the non-

reciprocal negative refraction appears and the nonreciprocal frequency band (see the shadow area in Fig. 3) becomes narrower with the increase of the temperature. Especially, the nonreciprocal negative refraction exists in a wide frequency range $[-0.01\gamma, 0.54\gamma]$ (see Fig. 3(a)) when the temperature reaches to 165 K. It can be explained as following. When the temperature increases, the depth and width of the EIT window dramatically reduce, and the electromagnetic response of the medium becomes weak so that the relative permeability amplitude decreases.[70] As the temperature is very high, the Doppler shifts get very large so that the EIT sate cannot exist in both directions and the relative permeability becomes positive in both cases as shown in Fig. 3(d). It results that negative refraction cannot be realized at very high temperature. In consequence, under appropriate temperature, nonreciprocal negative refraction can be obtained and the nonreciprocal band can be controlled by adjusting the temperature in our scheme.

In the following, we discuss the effect of the control field intensity Ω_{24} on the nonreciprocal negative refraction properties of the medium. The parameters are chosen as $\Omega_{13} = 0.16\gamma$, $T = 300$ K, and other parameters are the same as those in Fig. 2. Figure 4 shows the dependence of the real parts of the relative permittivity and relative permeability of the medium for the forward and backward probe field propagation with different control field intensities Ω_{24}. From Fig. 4, we find that the forward relative permeability is positive even if the relative permittivity is negative, then the atomic gas does not have left-handedness in forward propagation case. On the contrary, both of the relative permittivity and relative permittivity are negative in backward propagation case. So, the nonreciprocal negative refraction caused by the Doppler effect occurs in this hot medium. Furthermore, it is shown that the nonreciprocal frequency band (see the shadow area in Fig. 4) becomes narrow with the increase of the control field intensity Ω_{24}. Especially, when the control field $\Omega_{24} = 1.0\gamma$, the nonreciprocal negative refraction appears in a wide frequency range $[0, 0.50\gamma]$ (see Fig. 4(a)). It can be explained as following. As the Rabi frequency of the control field increases, the EIT window gradually increases and the magnetic dispersion slope curve becomes gently. It results in the decrease of the amplitude of the relative permittivity in the backward case. As a result, the nonreciprocal frequency band becomes narrow when the control field intensity increases. In addition, we find that the negative value of the backward relative permeability is positive and almost negligible corresponding to the control field $\Omega_{24} = 2.2\gamma$. At this time, there is no negative refraction in the forward and backward direction cases. Consequently, under appropriate intensity of the control field, we can obtain the nonreciprocal negative refraction and the nonreciprocal band can be adjusted by changing the intensity of the control field in this hot atomic medium.

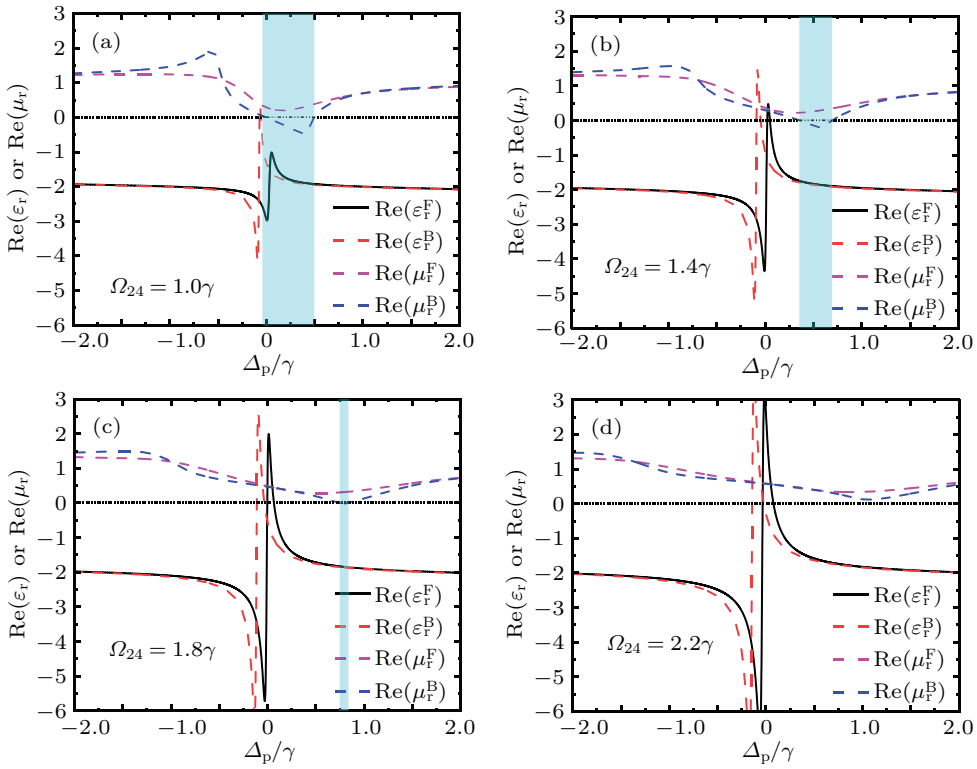


Fig. 4. The real part of the forward relative permittivity (black solid line) and permeability (magenta dotted line), the real part of the backward relative permittivity (red dashed line) and permeability (blue dash dot line) as a function of probe field detuning with different control field intensities Ω_{24}: (a) $\Omega_{24} = 1.0\gamma$, (b) $\Omega_{24} = 1.4\gamma$, (c) $\Omega_{24} = 1.8\gamma$, (d) $\Omega_{24} = 2.2\gamma$. The parameters are chosen as $\Omega_{13} = 0.16\gamma$ and $T = 300$ K, the other parameters are the same as those in Fig. 2.

In dense atomic gas, the local field effect should be considered, which is closely related to the atomic density.[71] In what follows, we analyze the effect of atomic density on nonreciprocal negative refraction. The parameters are chosen as $T = 300$ K, $\Omega_{13} = 0.12\gamma$, and the other parameters are the same as those in Fig. 2. As shown in Fig. 5, we plot the relative permeability and relative permittivity as a function of the probe field detuning with different atomic density in forward and backward cases. When the atomic density $N = 1.0 \times 10^{25}$ at/m^3, we find that the relative permeability is positive in both propagation directions and the negative refraction cannot exist (Fig. 5(a)). With the increase of atomic density N, the relative permeability in the backward case becomes negative so that the negative refraction appears in backward propagation but does not exist in the forward case. It results in the appearance of the nonreciprocal negative refraction (negative refraction exists in the backward case and does not exist in the forward case) with the gradual increase of atomic density N. It is because the local field effect becomes large with the increasing atomic density N, which could enhance the electromagnetic response to the medium and give rise to negative refraction. Particularly, as atomic density $N = 2.5 \times 10^{25}$ at/m^3, the width of the nonreciprocal interval $[-0.24\gamma, 0.55\gamma]$ reaches the maximum value. It is worth noting that the minimum value of the forward relative permeability is close to zero at this moment. It can be predicted that if the atomic density N is greater than 2.5×10^{25} at/m^3, the forward relative permeability will have a negative value, then the negative refraction appears in both directions, which is unfavorable for nonreciprocal negative refraction. Hence, under the suitable atomic density, we can realize nonreciprocal negative refraction and the nonreciprocal band can be manipulated by the atomic density.

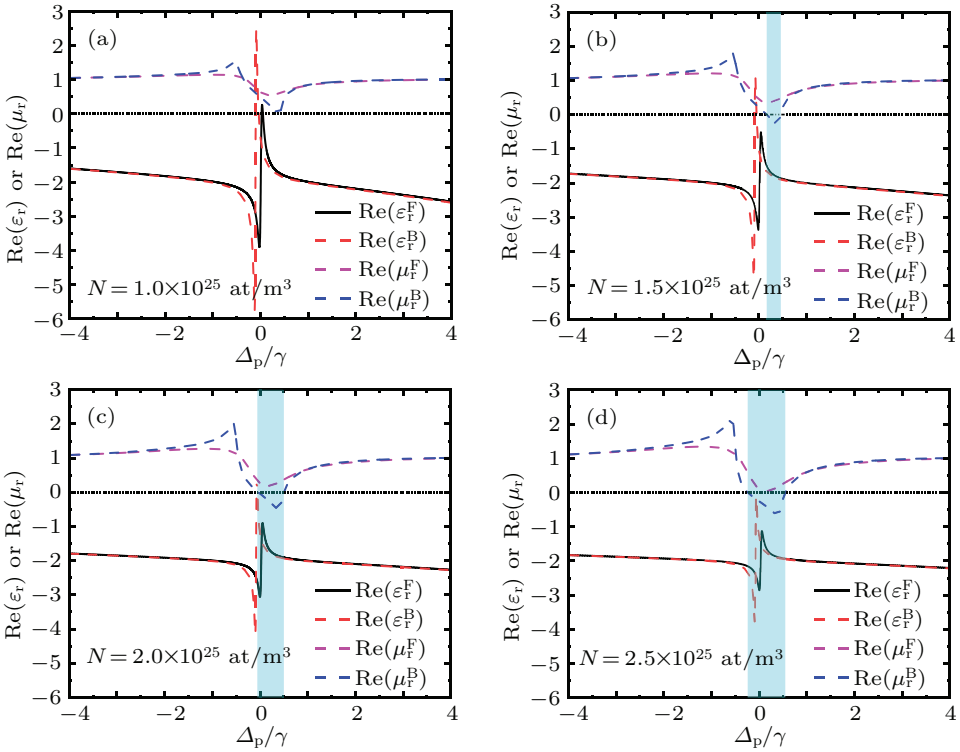


Fig. 5. The real part of the forward relative permittivity (black solid line) and permeability (magenta dotted line), the real part of the backward relative permittivity (red dashed line) and permeability (blue dash dot line) as a function of probe field detuning. (a) $N = 1.0 \times 10^{25}$ at/m^3, (b) $N = 1.5 \times 10^{25}$ at/m^3, (c) $N = 2.0 \times 10^{25}$ at/m^3, (d) $N = 2.5 \times 10^{25}$ at/m^3. The shaded area represents the nonreciprocal negative refraction interval. The parameters are $T = 300$ K, $\Omega_{13} = 0.12\gamma$, and the other parameters are the same as those in Fig. 2.

4. Conclusions

In summary, we propose a four-level scheme to induce nonreciprocal negative refraction by using the Doppler effect in a hot atomic medium. It is shown that, due to the Doppler effect, nonreciprocal negative refraction with less absorption can be realized at proper temperature. In addition, we find that the nonreciprocal frequency interval can be regulated by adjusting the temperature, the intensity of the control field and the atomic density. Our work may be used to realize unidirectional optical invisible and has potential applications in design of the photonic devices and optical communications.

Acknowledgements

Project supported by the National Natural Science Foundation of China (Grant No. 61671279). The authors also thank the financial support from Xi'an Key Laboratory of Optical Information Manipulation and Augmentation (OMA).

References

[1] Bi L, Hu J, Jiang P, Kim D H, Dionne G F, Kimerling L C and Ross C A 2011 *Nat. Photon.* **5** 758
[2] Ma S L, Ren Y L, Cao M T, Zhang S G and Li F L 2022 *Appl. Phys. Lett.* **120** 051109
[3] Shalaby M, Peccianti M, Ozturk Y and Morandotti R 2013 *Nat. Commun.* **4** 1558
[4] Tamagnone M, Moldovan C, Poumirol J M, Kuzmenko A B, Ionescu A M, Mosig J R and Perruisseau-Carrier J 2016 *Nat. Commun.* **7** 11216
[5] Estep N A, Sounas D L, Soric J and Alù A 2014 *Nat. Phys.* **10** 923
[6] Kamal A, Clarke J and Devoret M H 2011 *Nat. Phys.* **7** 311
[7] Shen Z, Zhang Y L, Chen Y, Sun F W, Zou X B, Guo G C, Zou C L and Dong C H 2018 *Nat. Commun.* **9** 1797
[8] Zheng J H, Peng R, Cheng J, An J and Zhang W Z 2022 *Chin. Phys. B* **31** 054204
[9] Khanikaev A B, Mousavi S H, Shvets G and Kivshar Y S 2010 *Phys. Rev. Lett.* **105** 126804
[10] Tse W K and MacDonald A H 2011 *Phys. Rev. B* **84** 205327
[11] Bender N, Factor S, Bodyfelt J D, Ramezani H, Christodoulides D N, Ellis F M and Kottos T 2013 *Phys. Rev. Lett.* **110** 234101
[12] Khanikaev A B and Alù A 2015 *Nat. Photon.* **9** 359
[13] Sounas D L, Soric J and Alù A 2018 *Nat. Electron.* **1** 113
[14] Rosario Hamann A, Muller C, Jerger M, Zanner M, Combes J, Pletyukhov M, Weides M, Stace T M and Fedorov A 2018 *Phys. Rev. Lett.* **121** 123601
[15] Feng L, Ayache M, Huang J, Xu Y L, Lu M H, Chen Y F, Fainman Y and Scherer A 2011 *Science* **333** 729
[16] Lira H, Yu Z, Fan S and Lipson M 2012 *Phys. Rev. Lett.* **109** 033901
[17] Sounas D L and Alù A 2017 *Nat. Photon.* **11** 774
[18] Yu Z and Fan S 2009 *Nat. Photon.* **3** 91
[19] Ruesink F, Miri M A, Alu A and Verhagen E 2016 *Nat. Commun.* **7** 13662
[20] Mercier de Lépinay L, Damskägg E, Ockeloen-Korppi C F and Sillanpää M A 2019 *Phys. Rev. Appl.* **11** 034027
[21] Manipatruni S, Robinson J T and Lipson M 2009 *Phys. Rev. Lett.* **102** 213903
[22] Fang K, Luo J, Metelmann A, Matheny M H, Marquardt F, Clerk A A and Painter O 2017 *Nat. Phys.* **13** 465
[23] Horsley S A, Wu J H, Artoni M and La Rocca G C 2013 *Phys. Rev. Lett.* **110** 223602
[24] Ramezani H, Jha P K, Wang Y and Zhang X 2018 *Phys. Rev. Lett.* **120** 043901
[25] Wu J H, Artoni M and La Rocca G C 2014 *Phys. Rev. Lett.* **113** 123004
[26] Wang D W, Zhou H T, Guo M J, Zhang J X, Evers J and Zhu S Y 2013 *Phys. Rev. Lett.* **110** 093901
[27] Sollner I, Mahmoodian S, Hansen S L, Midolo L, Javadi A, Kirsanske G, Pregnolato T, El-Ella H, Lee E H, Song J D, Stobbe S and Lodahl P 2015 *Nat. Nanotechnol.* **10** 775
[28] You Y, Hu Y, Lin G, Qi Y, Niu Y and Gong S 2021 *Phys. Rev. A* **103** 063706
[29] Xia K, Lu G, Lin G, Cheng Y, Niu Y, Gong S and Twamley J 2014 *Phys. Rev. A* **90** 043802
[30] Shi C, Cheng M T, Ma X S, Wang D, Huang X, Wang B and Zhang J Y 2018 *Chin. Phys. Lett.* **35** 054202
[31] Hu Y, Zhang S, Qi Y, Lin G, Niu Y and Gong S 2019 *Phys. Rev. Appl.* **12** 054004
[32] Zhang S, Lin G, Hu Y, Qi Y, Niu Y and Gong S 2020 *Phys. Rev. Appl.* **14** 024032
[33] Lu X, Cao W, Yi W, Shen H and Xiao Y 2021 *Phys. Rev. Lett.* **126** 223603
[34] Zhang S, Hu Y, Lin G, Niu Y, Xia K, Gong J and Gong S 2018 *Nat. Photon.* **12** 744
[35] Brandenbourger M, Locsin X, Lerner E and Coulais C 2019 *Nat. Commun.* **10** 4608
[36] Shen Z, Zhang Y L, Chen Y, Zou C L, Xiao Y F, Zou X B, Sun F W, Guo G C and Dong C H 2016 *Nat. Photon.* **10** 657
[37] Lin G, Zhang S, Hu Y, Niu Y, Gong J and Gong S 2019 *Phys. Rev. Lett.* **123** 033902
[38] Fan L, Wang J, Varghese L T, Shen H, Niu B, Xuan Y, Weiner A M and Qi M 2012 *Science* **335** 447
[39] Veselago V G 1968 *Sov. Phys. Usp.* **10** 509
[40] Berman P R 2002 *Phys. Rev. E* **66** 067603
[41] Pendry J B 2016 *J. Phys.: Condens. Matter* **28** 481002
[42] Chen L, He S and Shen L 2004 *Phys. Rev. Lett.* **92** 107404
[43] Aydin K, Bulu I and Ozbay E 2007 *Appl. Phys. Lett.* **90** 254102
[44] Pendry J B 2000 *Phys. Rev. Lett.* **85** 3966
[45] Schurig D, Mock J J, Justice B J, Cummer S A, Pendry J B, Starr A F and Smith D R 2006 *Science* **314** 977
[46] Smith D R, Padilla W J, Vier D C, Nemat-Nasser S C and Schultz S 2000 *Phys. Rev. Lett.* **84** 4184
[47] Shelby R A, Smith D R and Schultz S 2001 *Science* **292** 77
[48] Yen T J, Padilla W J, Fang N, Vier D C, Smith D R, Pendry J B, Basov D N and Zhang X 2004 *Science* **303** 1494
[49] Linden S, Enkrich C, Wegener M, Zhou J, Koschny T and Soukoulis C M 2004 *Science* **306** 1351
[50] Enkrich C, Wegener M, Linden S, Burger S, Zschiedrich L, Schmidt F, Zhou J F, Koschny T and Soukoulis C M 2005 *Phys. Rev. Lett.* **95** 203901
[51] Berrier A, Mulot M, Swillo M, Qiu M, Thylen L, Talneau A and Anand S 2004 *Phys. Rev. Lett.* **93** 073902
[52] He S, Ruan Z, Chen L and Shen J 2004 *Phys. Rev. B* **70** 115113
[53] Cubukcu E, Aydin K, Ozbay E, Foteinopoulou S and Soukoulis C M 2003 *Nature* **423** 604
[54] Wu H, Jiang L Y, Jia W and Li X Y 2012 *Chin. Phys. Lett.* **29** 034203
[55] Yu X T, Wei Z Y, Li H Q, Zhang Y W and Chen H 2007 *Chin. Phys. Lett.* **24** 3447
[56] Pendry J B 2004 *Science* **306** 1353
[57] Yannopapas V 2006 *J. Phys.: Condens. Matter* **18** 6883
[58] Tretyakov S, Sihvola A and Jylhä L 2005 *Photon. Nanostruct. Fundam. Appl.* **3** 107
[59] Oktel M Ö and Müstecaplıoğlu Ö E 2004 *Phys. Rev. A* **70** 053806
[60] Shen J Q, Ruan Z C and He S L 2004 *J. Zhejiang Univ. Sci.* **5** 1322
[61] Zhang H J, Gong S Q, Niu Y P, Li R X and Xu Z Z 2006 *Chin. Phys. Lett.* **23** 1769
[62] Shen J Q 2006 *Phys. Lett. A* **357** 54
[63] Thommen Q and Mandel P 2006 *Phys. Rev. Lett.* **96** 053601
[64] Kastel J, Fleischhauer M, Yelin S F and Walsworth R L 2007 *Phys. Rev. Lett.* **99** 073602
[65] Kästel J, Fleischhauer M, Yelin S F and Walsworth R L 2009 *Phys. Rev. A* **79** 063818
[66] Yang X Y and Jiang Y Y 2012 *Opt. Commun.* **285** 2161
[67] Zhao S C, Liu Z D and Wu Q X 2010 *Opt. Commun.* **283** 3301
[68] Zhao S C, Liu Z D, Zheng J, Li G and Liu N 2012 *Optik* **123** 1063
[69] Jackson J D 2001 *Classical Electrodynamics* 3rd edn. (New York: John Wiley & Sons) Chap. 4
[70] Van Ai N, Bang N H and Van Doai L 2022 *Phys. Scr.* **97** 025503
[71] Friedberg R, Hartmann S R and Manassah J T 1989 *Phys. Rev. A* **40** 2446